R4-B.4: Integrated Reconstruction/Recognition

I. PARTICIPANTS

Faculty/Staff			
Name	**Title**	**Institution**	**Email**
Clem Karl	Co-PI	BU	wckarl@bu.edu
David Castañón	Co-PI	BU	dac@bu.edu
Limor Martin	Post-doc	BU	limor@bu.edu

II. PROJECT DESCRIPTION

A. Overview and Significance

In CT-based security screening, a challenging problem is to correctly identify and label objects in a scene from X-ray projection data. Conventionally, material parameter reconstruction and labelling are performed as two decoupled steps. Image artifacts induced from metal and other clutter cause variations in apparent material density as well as streaking that can break up homogeneous objects, making their correct identification and assessment challenging. In this project, methods are developed that incorporate the tools of machine learning, physical modeling and Bayesian inference into a unified framework for direct material identification and labeling. Reliable material labelling is critical to the efficient operation of the checkpoint, which is made extremely challenging due to the large range of objects that can appear in baggage, the presence of high clutter, and metal induced image artifacts. The new approach that has been developed can mitigate image artifacts and robustly label materials, thus reducing the number of corner cases, which can in turn reduce false alarms and the need for On-Screen Alarm Resolution Protocol (OSARP) and manual inspection.

B. State-of-the-Art and Technical Approach

A challenging problem in CT-based screening is finding and labeling objects of interest in the scene [1-5]. Traditional approaches perform decoupled steps in obtaining material labels. The first step performs image processing, such as filtering and denoising, in an attempt to reduce noise and image artifacts. These processed images are then labeled or segmented in an attempt to find objects and determine their underlying materials cut [12, 13]. We have developed a new direct, dictionary-based method for material labeling from Multi-Energy Computed Tomography (MECT) measurements. This new method takes into account the system model information together with a dictionary-based model of the measured sinograms. The linear attenuation coefficients (LACs) of the materials of interest are used as dictionary elements. The typically decoupled approach and the new proposed joint approach are illustrated in Figure 1.

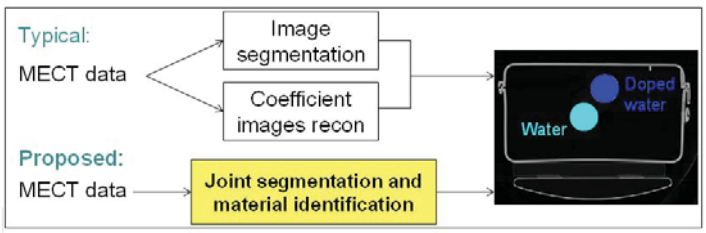

Figure 1: Object segmentation and labeling: decoupled (typical) versus joint (proposed) paths.

The observed normalized log-sinogram data in MECT sensing follows the non-linear Beer-Lambert law of X-ray imaging [8-10]:

$$I_s(\ell) = -\ln\left(\frac{\int w_s(E) e^{-\int_\ell \mu(x,E)\,dx}\,dE}{\int w_s(E)\,dE}\right)$$

where $I_s(\ell)$ is the measurement along ray-path ℓ for spectral weighting s, $w_s(E)$ is the spectral weighting function S used in the measurement, and $\mu(x, E)$is the LAC of the material at spatial location X and energy E, which identifies the material present at that location. Examples of LAC curves and spectral weighting functions are shown in Figure 2.

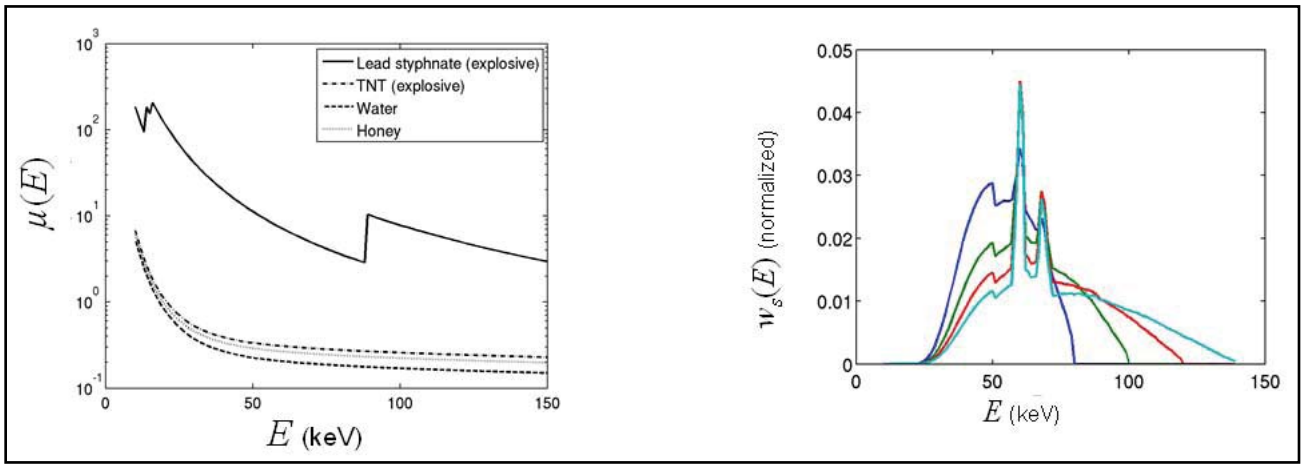

Figure 2: Left: the linear attenuation coefficient (LAC) curves of a few example materials. Right: examples of spectral weighting functions $w_s(E)$ used in X-ray based sensing (normalized to unit sum).

The characteristics of the material at spatial location X are captured through the energy dependent function $\mu(x, E)$. Typically, this function is approximated as a linear combination of only two basis functions [11], such as the photoelectric and Compton basis functions. In the security application, however, we are less concerned with accurate representation of the function than with accurate identification of the material at that spatial location. In this work we focus on this identification aspect.

Initially, we developed a first principle physics-based approach starting from the MECT projection data for the estimation of the material label image. The approach takes into account the tomographic system model through the Beer-Lambert law. The novel component is that a dictionary-based model of the materials of interest in the scene is used, with the LACs of materials of interest used as the dictionary elements. Dictionary coefficients are estimated using a sparsity constraint and then used to identify material labels that match the observed multi-energy observations. A Markov random field (MRF) type model, which captures our belief that the label field should display spatial coherence, is used to suppress artifacts. This spatial coherence reflects the behavior of objects in the scene and serves to further our goal of preventing the splitting of objects.

Specifically, we create a dictionary of LACs of the few materials of interest:

$$D = [\mu_1 \quad \mu_2 \quad \cdots \quad \mu_m]$$

where μ_k is a vector representing the LAC of material label k as a function of (discretized) energy level. This dictionary provides an overcomplete basis for representing the material LAC in the scene. Let c_x be the LAC

composition vector for the pixel at location x in the scene. The LAC of the material at pixel location x is then given by the linear combination of dictionary elements specified by the product Dc_x. Since we believe there is only a single material at pixel x, we assume sparsity of the vectors c_x such that only a single entry of c_x will be 1 and the rest 0. We find the material labels by solving a unified optimization problem with this dictionary-based scene model under the previous Beer-Lambert X-ray observations. The overall formulation is:

$$\min_{\substack{(c_1,c_2,\ldots,c_N)\\ \|c_i\|_0=1\\ \|c_i\|_2=1}} \left\{ \sum_{s,r} \left[-\ln\left(\frac{\int w_s(E) e^{-\int_{\ell_r} Dc_x(E)dx} dE}{\int w_s(E)dE} \right) - I_s(\ell_r) \right]^2 + \lambda \psi_{MRF}(c_1,c_2,\ldots,c_N) \right\}$$

The first summation in the formula above is a data fidelity term. It is defined as the squared error between the measured sinogram and the dictionary-based model based on the physical Beer-Lambert law. The second term is a Potts-type MRF prior term. This term penalizes any differences in dictionary coefficient vectors for pixels in a small neighborhood. Different coefficient vectors correspond to different labels and the desire is to increase the coherency of the label field. The minimization is performed subject to the constraints that only a single entry of any coefficient vector c_x at spatial location x is equal to 1. These constraints reflect the belief that there is only one material at each spatial location, and that this material is associated to a particular column of the material dictionary D. A solution is obtained by an iterative process that solves for each c_x in sequence while keeping the others fixed. All the material possibilities are tested and the one that provides the lowest value of the cost function is selected. Note that this new approach is performing direct, integrated segmentation and labeling in contrast to conventional ad-hoc multi-step processes. We call this method the "dictionary labeling" method.

While the above dictionary labeling method exploits the complete physical sensing model as well as knowledge of material X-ray behavior and scene construction through a dictionary, it requires detailed knowledge of system parameters, such as sensing geometry, spectral shapes, material LACs, etc., and can be computationally demanding because repeated tomographic mappings are required in its solution. As a result, a more recent thrust of our research in this project has focused on the development of efficient data-driven approaches using machine learning and graph-cut methods [14]. In this second approach, we start from conventionally formed effective attenuation images for each multi-energy experiment, which are natively available, and then directly learn the conditional appearance model for each material of interest from a set of such training data. As a result, explicit physical models of the complete tomographic system and detailed information on material LACs are not needed. Given this learned multi-energy appearance model, a discrete label-based optimization is performed for material type. The optimization functional includes prior knowledge of the nature of typical security image artifacts, allowing for their suppression.

To develop the method, let $\bar{\mu}^H$ and $\bar{\mu}^L$ denote the conventionally created effective attenuation images for a high energy and low energy X-ray CT scan, respectively. Extension to more than two energies is straight forward. At any spatial location x, the appearance of a material in these two scans is modeled as a probability density

$$p\left(\begin{bmatrix} u_{H,x} \\ u_{L,x} \end{bmatrix} \middle| l_x \right)$$

conditioned on the label l_x of the material at that location. This density captures the potential variability in material appearance and is directly found using machine learning kernel density estimation techniques from training data. In this way, the method directly captures appearance uncertainty and does not require detailed or explicit physical material or scanner knowledge.

Unfortunately, conventionally created effective attenuation images may contain streaks [7], which cause the splitting of objects and shading, resulting in the corruption of attenuation values. The probabilistic appearance model can capture and model a portion of this variability, providing some mitigation, but direct incorporation of additional prior information can improve the final result. For example, a large source of artifacts in luggage scans is the presence of metal objects. Further, such metal artifacts are often stronger the closer the pixels are to the metal object. To reflect this insight, observed data near metal objects is assumed less reliable and, therefore, down weighted. In addition, to prevent object splitting and reduce attenuation variability in homogeneous regions, an object boundary field is used.

Overall, material labels at each pixel location and segmentation of objects is obtained jointly as the solution of the following optimization problem:

$$\min_{(l_1,l_2,\ldots,l_N)} \left\{ \sum_x v_x \left(-\ln p\left(\begin{bmatrix} \bar{\mu}_j^L \\ \bar{\mu}_j^H \end{bmatrix} \middle| l_x \right) \right) + \lambda g_{MRF}(l_1,l_2,\ldots,l_N,s) \right\}$$

$$\text{subject to } \; l_x \in \{1,2,\ldots,M\} \; \forall x$$

In this framework $\bar{\mu}^H$ and $\bar{\mu}^L$ are the conventionally formed effective attenuation images obtained from measurements with two different (high and low) spectral weightings, l_x is the material label at pixel x,

$$p\left(\begin{bmatrix} u_{1,x} \\ u_{2,x} \end{bmatrix} \middle| l_x \right)$$

is the learned appearance model for material label l_x at pixel x, v_j are data weights which down-weight data points in the vicinity of metal, λ is a non-negative regularization parameter and $g_{MRF} = (l_1, l_2, \ldots l_N, s)$ is an MRF smoothing term, which is based on an estimate of the image boundary field S. This MRF model captures local coherence of material labels and takes into account an estimate of object boundaries to further ensure label homogeneity within an object. Figure 3 on the next page shows the main components of the method for an example slice from the Imatron scans database. The resulting optimization problem is a non-convex, discrete label problem, which are, in general, challenging to solve. To accomplish this optimization, an efficient graph-cut based method has been developed. Such graph-cut methods have been popular in the computer vision land discrete optimization literature, but have not been used in this domain. These methods map the original optimization problem to an equivalent graph flow problem and a minimal cut of this graph provides the optimal solution. These methods have shown great success in producing efficient near optimal solutions for very challenging discrete problems, and are well suited to our application. We call this overall method "learning-based object identification and segmentation" or LOIS.

In contrast to existing methods, LOIS incorporates machine learning methods for appearance model generation, obviating the need for complex tomographic models. LOIS includes prior knowledge of security-based artifact behavior, reducing splitting and shading and, thus, reducing false labelling. LOIS also directly generates material labels through an inherently discrete, label-based solution built on efficient graph-cut methods.

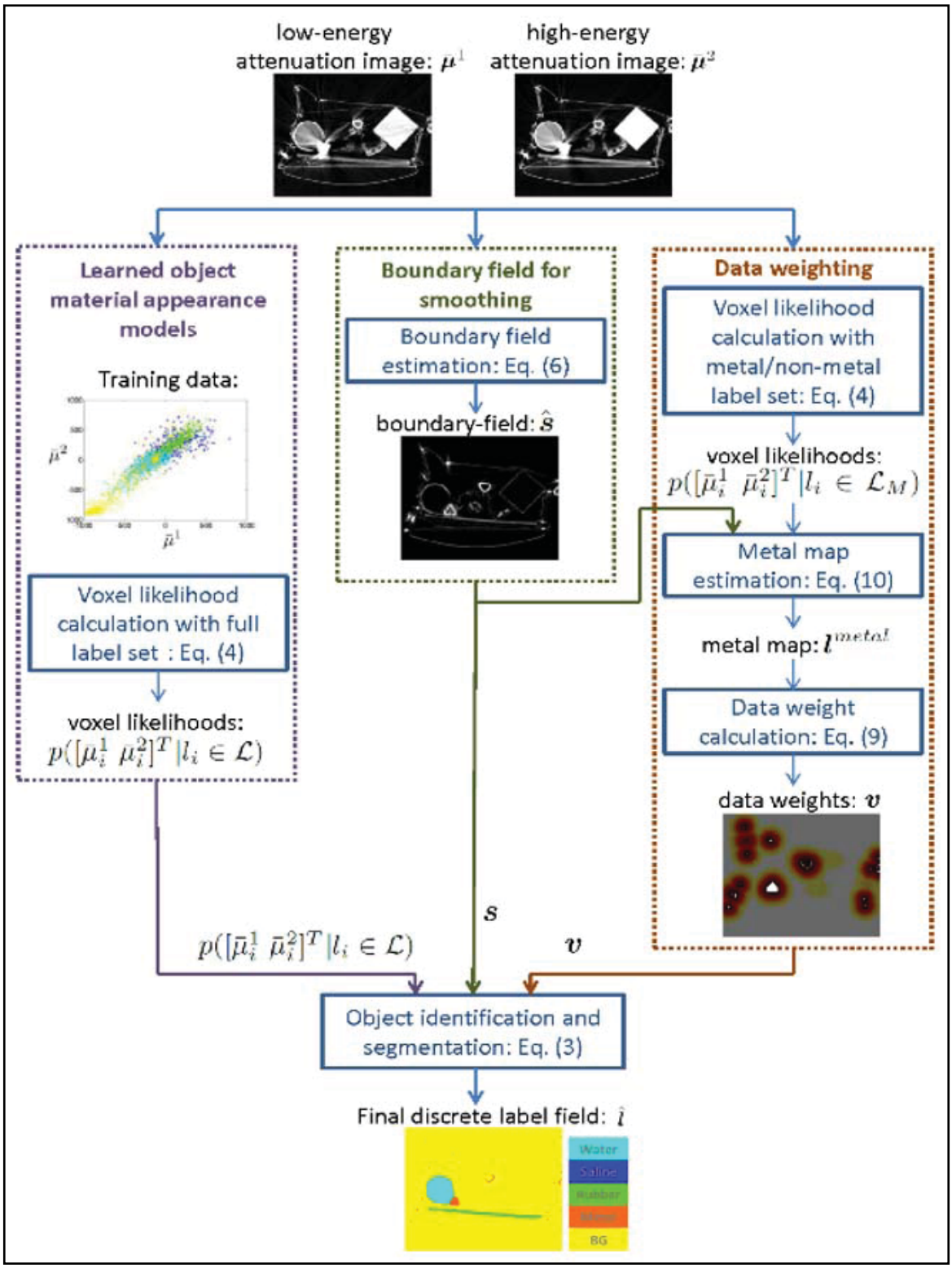

Figure 3: Illustration of the main components of the learning-based graph-cut labeling method. The left column generates the learned appearance models, which account for variability and materials of interest. The middle column generates an object boundary field, used in the smoothing term. The right column generates a map of metal and corresponding metal-sensitive data weights. Data points close to metal are given lower weights. All three components are used in the overall graph-cut based optimization at the bottom.

C. Major Contributions

We have developed and tested our new methods for robust material identification from multi-energy X-ray sensed data. Using LOIS, we have developed a robust and efficient learning-based method for direct material labeling from multi-energy data sets. This method exploits the physics of multi-energy imaging and the power of machine learning. An integrated framework incorporating prior knowledge of artifact behavior reduces false alarms. Direct labeling is accomplished through a graph-cut based optimization approach.

We tested our methods by creating direct labeling of material from dual-energy CT data. We implemented the methods described above and tested them on real dual-energy data from the Imatron scans database obtained under ALERT Task Order 3 (TO3). These are dual-energy scans of different objects in bags obtained with 95 kVp and 130 kVp source spectra.

For the dictionary labeling method, we constructed a dictionary with the LACs of graphite, magnesium and silicon, providing four possible material labels: graphite, magnesium, silicon and background (air). We applied the method to a scan slice that had graphite, magnesium and silicon rods, which were placed in foam inside of a plastic case. The results are shown in Figure 4. The labeling results seem to be accurate and we see that the MRF prior helps maintain object homogeneity.

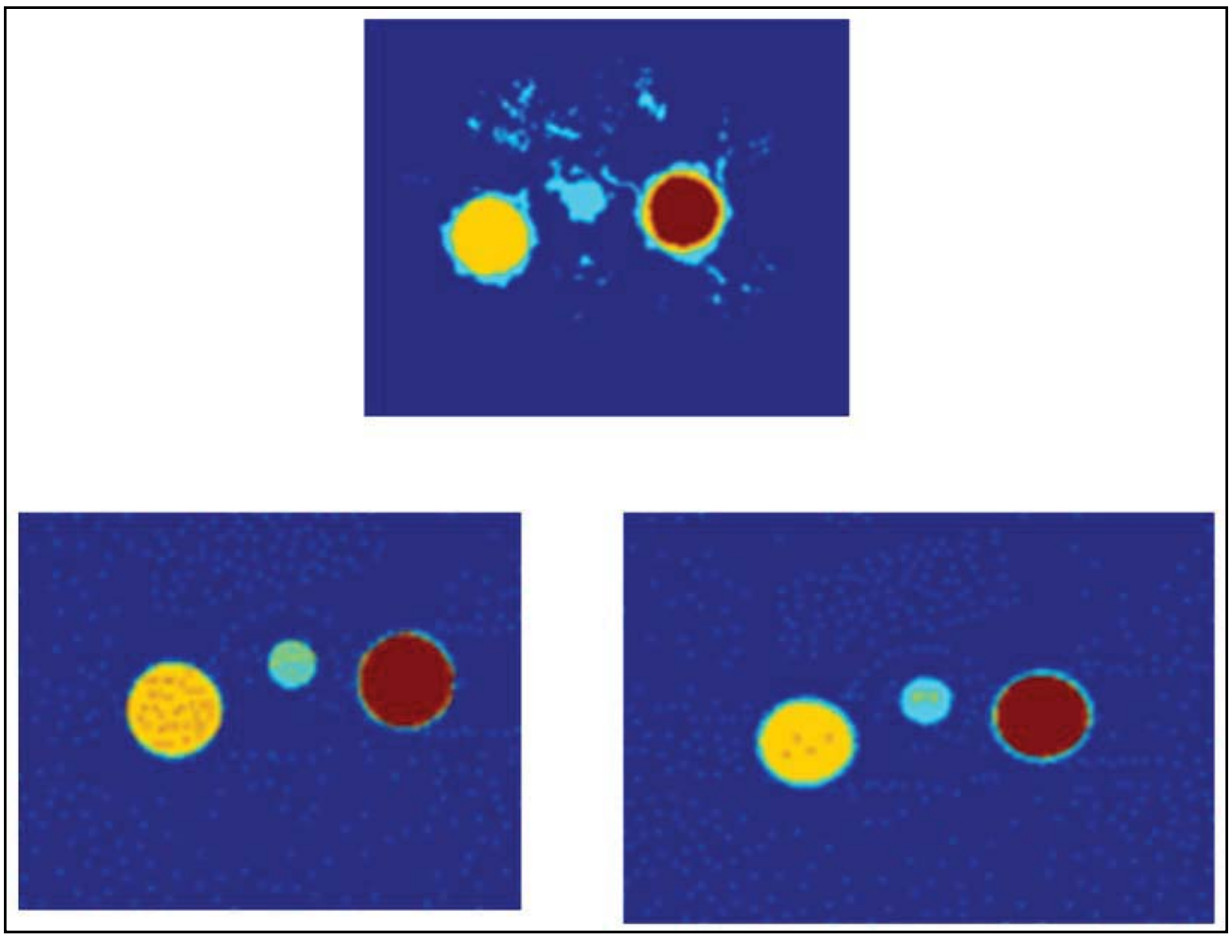

Figure 4: Material label images using the dictionary labeling method for a slice with graphite, magnesium and silicon rods placed in foam inside of a plastic container. The magnesium rod is on the left, the graphite rod is in the middle and silicon is on the right. The dictionary was composed of graphite, magnesium and silicon LACs. Graphite is labeled in light blue, magnesium is labeled in yellow, silicon is labeled in red and background is labeled in dark blue. Top: initialization. Bottom left: result with no MRF prior. Bottom right: result with an MRF prior. The method achieves accurate material labeling and, using the MRF prior, helps to get more homogeneous results.

For the LOIS learning-based graph-cut labeling method, in this period, we have extended our preliminary 2D slice-by-slice results to a fully 3D solution and compared it to a conventional K-nearest neighbor (KNN) classifier trained with the same data. Training data was obtained for the following material labels: water, doped water, rubber and metal. Everything else was treated as an "other" category, which included background, air and unmodeled materials. The learning-based method automatically creates an appearance model for these things. Figure 5 shows a typical result from the Imatron data. On the left are cross-sections of the original high-energy input image. In the middle are the results obtained from a conventional KNN labeling approach. On the right are the results obtained with LOIS. In these images, water is dark blue, doped water is light blue, rubber is green, metal is orange and background is yellow. Despite the presence of metal and its associated streak artifacts, as well as significant clutter materials, the object materials of interest, in this case rubber sheet objects and doped and undoped water (blue shades), are correctly labeled without splitting or breaks. Overall, image quality is greatly improved.

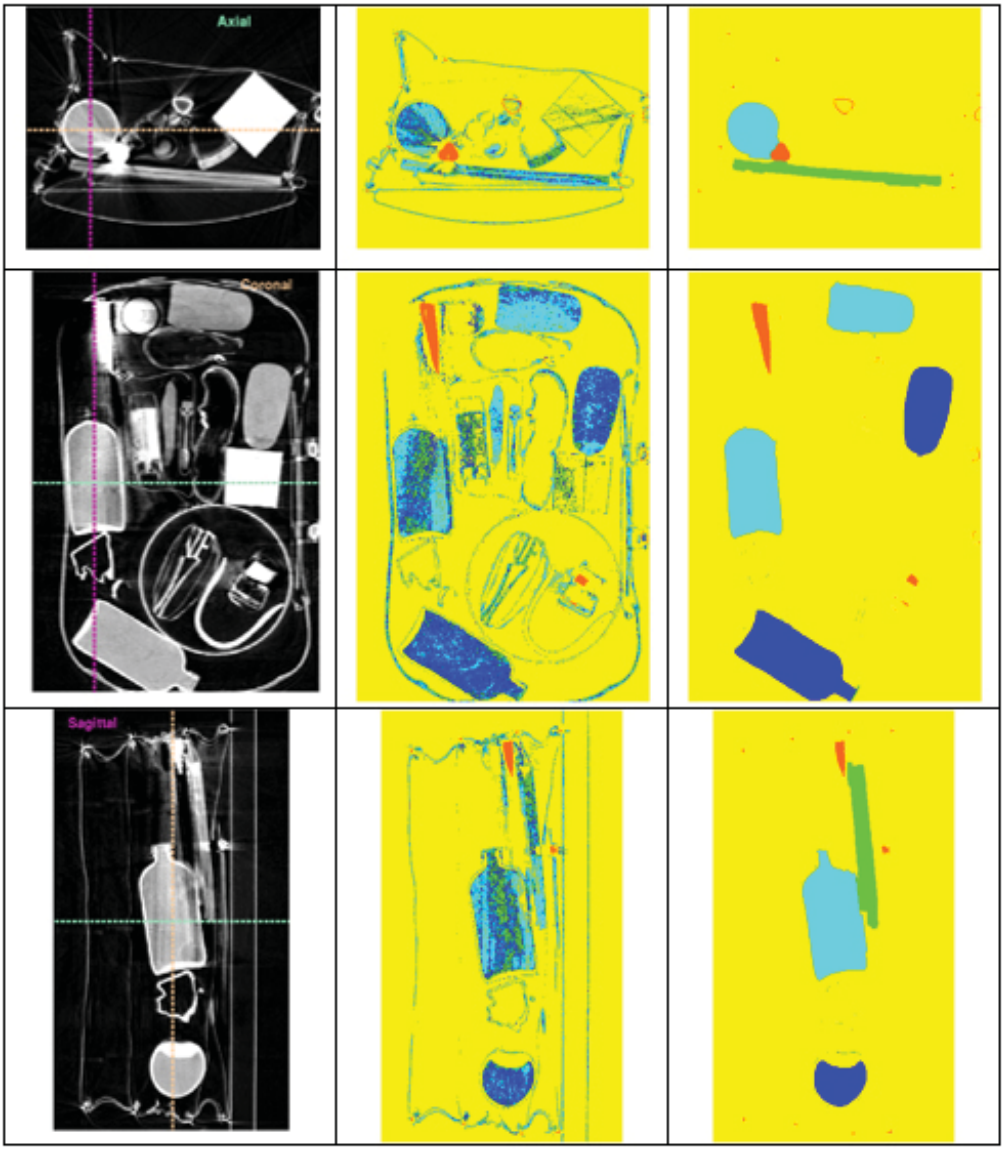

Figure 5: Original 130kVp image cross-sections (left column), conventional KNN labeled cross-sections (middle column) and LOIS labeled cross-sections (right column). Water is dark blue, doped water is light blue, rubber is green, metal is orange and background is yellow. Rubber sheets and water bottles are correctly found despite metal streaks and significant clutter.

Overall, these methods provide physics-based principled approaches for direct material labeling in the face of a large clutter class that contrasts current ad hoc, two-step decoupled approaches. The potential gain of such optimal methods are reduced artifacts, lower false alarms and improved material labeling.

D. Milestones

The project as originally envisioned has reached the following major milestones:

1. Theoretical formulation of a novel integrated learning-based classification framework for dual-energy CT with integrated artifact mitigation;
2. Initial controlled simulations to validate the concept and refine formulation;
3. Application to single slice dual-energy images using TO3 datasets
4. Extension of the method from 2D to a fully 3D approach; and
5. Application of the method to multi-energy volumetric image data from TO3.

E. Future Plans

Our future plan is to merge the robust learning-based automated recognition work under R4-B.4 with the artifact mitigation developments under R4-C1 and focus on a new direction motivated by advanced X-ray-based checkpoint screening. In particular, this new direction would aim to address current limitations identified, for example, in TSA RFI HSTS04-15-RFI-CT7999 together with the requirements for the next generation checkpoint. These goals include enhanced screening with lower false alarms, higher throughput and automated target identification. In addition, these goals need to be met with limited scanner footprint, weight and cost. To accomplish this, scanners will need to create 3D images from limited numbers of views and utilize novel, non-rotational geometries. We propose to incorporate the lessons learned from our previous projects to develop new algorithms for highly-limited-view tomographic reconstruction, artifact suppression and unified learning-based object identification based on compressed sensing and coded-aperture methods coupled with powerful optimization solver approaches, such as ADMM. We will exploit and adapt our previous work on non-conventional, limited geometry synthetic aperture radar reconstruction to these challenging security problems. One aspect of this work will focus on reducing the number of projection views needed for satisfactory reconstruction quality through the use of sparsity and compressed sensing methodologies. Another aspect of this work will focus on development of robust material models from training data.

III. EDUCATION AND WORKFORCE DEVELOPMENT ACTIVITY

A. Course, Seminar or Workshop Development

Special session for ICIP 2015 on Computational Imaging is being developed.

Graduate course on image formation called “Image reconstruction and restoration” was conducted with 15 enrolled students.

B. Other outcomes that relate to educational improvement or workforce development

Ahmet Tuysuzoglu graduated with his PhD in Electrical and Computer Engineering in 2014 from Boston University. He is now working as a research scientist at Siemens Corporate Research.

IV. RELEVANCE AND TRANSITION

A. Relevance of Research to the DHS Enterprise

This project is of relevance to the DHS enterprise because it is developing methods to mitigate image artifacts in an effort to cope with the large and unstructured class of clutter materials in baggage in multi-spectral CT scanning. These approaches can reduce the number of corner cases and false alarms, which in turn can reduce the need for OSARP and manual inspection. These concerns will grow as the use of multi-spectral X-ray scanning increases at the checkpoint.

B. Potential for Transition

Interest at TSA, TSL & DHS EXD for evaluation on CT explosives data. For example, R. Krauss from TSL has expressed interest in evaluating the LOIS method.

C. Data and/or IP Acquisition Strategy

Data from the Imatron scanner acquired under TO3 were used for demonstration and validation.

D. Transition Pathway

The novel methods developed in this effort have been disseminated to vendors through workshops and prior student engagement in summer internships. Vendors could incorporate the methods being developed in this project into their ATR chains. Several vendors at the symposium for the TO3 "Research and Development of Reconstruction Advances in CT-based Object Detection Systems" effort supported by DHS Task Order Number HSHQDC-10-J00396, (e.g. L3) commented that they had not thought that results this good could be obtained directly from dual-energy data. In addition, TSL/S&T personnel (C. Love, R. Krauss, and R. Klueg) expressed interest in collaborating with us to see how well these methods would perform on laboratory material samples.

E. User Connections

TSL/S&T personnel (R. Krauss) expressed renewed interest in collaborating with us to see how these methods would perform on laboratory material samples presented at the twelfth Advanced Development for Security Applications workshop (ADSA12).

V. PROJECT DOCUMENTATION

A. Peer Reviewed Journal Articles

1. A. Tuysuzoglu, W. C. Karl, I. Stojanovic, D. A. Castanon, and S. Unlu, ``Graph-cut based Discrete-Valued Image Reconstruction,'' IEEE Trans. on Image Processing, Vol. 24, No. 5, May, 2015.
2. L. Martin, A. Tuysuzoglu, W. C. Karl, P. Ishwar, ``Learning-based object identification and segmentation using dual-energy CT images for security,'' IEEE Trans. on Image Processing, Vol 24, No. 11, 2015.

B. New and Existing Courses Developed and Student Enrollment

New or Existing	Course/Module/ Degree/Cert.	Title	Description	Student Enrollment
Existing	Course	Image reconstruction and restoration	Graduate course on image formation	15

C. Software Developed

1. Datasets
   a. TO3 and TO4 Data resources

VI. REFERENCES

[1] K. Wells and D. Bradley, "A review of x-ray explosives detection techniques for checked baggage," Appl. Radiat. Isotopes, vol. 70, no. 8, pp. 1729 – 1746, 2012.
[2] Crawford, C., Martz, H., and Karl, W. C., "Research and development of reconstruction advances in CT-based object detection systems – final report," tech.rep., ALERT DHS Center of Excellence (2013).
[3] N. E. Shanks and A. L. Bradley, Handbook of Checked Baggage Screening: Advanced Airport Security Operation. John Wiley & Sons, 2005.
[4] K.W. Dolan, R.W. Ryon, D.J. Schneberk, H.E. Martz, R.D. Rikard, Explosives detection limitations using dual-energy radiography and computed tomography, Proceedings of the First International Symposium on Explosives Detection Technology, 1991, pp. 252–260
[5] S. Singh and M. Singh, Explosives detection systems (EDS) for aviation security, Signal Processing 83 (2003), 31–55.
[6] J. Heismann, J. Leppert and K. Stierstorfer, Density and atomic number measurements with spectral X-ray attenuation method J. Appl. Phys 94 2073-9, 2003.
[7] De Man, J. Nuyts, P. Dupont, G. Marchal, and P. Suetens, "Metal streak artifacts in X-ray computed tomography: a simulation study," IEEE Tr. Nuc. Sci. 46, pp. 691–6, June 1999.
[8] Macovski, A. (1983). Medical Imaging Systems. Prentice-Hall.
[9] Alvarez, R. E. and Macovski, A. (1976). Energy-selective reconstruction in X-ray computerized tomography. Physics in Medicine and Biology, 21(5):733-744.
[10] Z.Ying, R. Naidu, and C. Crawford, Dual energy computed tomography for explosive detection, J. of X-ray Sci. and Tech., vol. 14, no. 4, pp. 235–256, 2006.
[11] J. A. Fessler, I. A. Elbakri, P. Sukovic, and N. H. Clinthorne, "Maximum-likelihood dual-energy tomographic image reconstruction," In Proc. SPIE 4684, Medical Imaging 2002: Image Proc., 2002.
[12] D. F. Wiley, D. Ghosh, and C. Woodhouse, "Automatic segmentation of CT scans of checked baggage," in Proc. of the 2nd Inter. Meeting on Image Formation in X-ray CT, June 2012, pp. 310–313.
[13] L. Grady, V. Singh, T. Kohlberger, C. Alvino, and C. Bahlmann, "Automatic segmentation of unknown objects, with application to baggage security," in European Conference on Computer Vision (ECCV), Oct. 2012, pp. 430–444.
[14] Y. Boykov, O. Veksler, and R. Zabih, "Fast approximate energy minimization via graph cuts," IEEE Trans. Pattern Anal. Mach. Intell., vol. 23, no. 11, pp. 1222–1239, 2001.